Pergamon

Geochimica et Cosmochimica Acta, Vol. 65, No. 5, pp. 777–789, 2001

0016-7037/01 $20.00 + .00

PII S0016-7037(00)00579-2

Fractionation of sulfur isotopes during bacterial sulfate reduction in deep ocean sediments at elevated temperatures

MARK D. RUDNICKI,[1,*,†] HENRY ELDERFIELD,[1] and BARUCH SPIRO[2]

[1]Department of Earth Sciences, University of Cambridge, Downing Street, Cambridge CB2 3EQ, UK
[2]NERC Isotope Geosciences Laboratory, Keyworth, Nottingham NG12 5GG, UK

(*Received March* 11, 2000; *accepted in revised form October* 2, 2000)

Abstract—A numerical model of sulfate reduction and isotopic fractionation has been applied to pore fluid SO_4^{2-} and $\delta^{34}S$ data from four sites drilled during Ocean Drilling Program (ODP) Leg 168 in the Cascadia Basin at 48°N, where basement temperatures reach up to 62°C. There is a source of sulfate both at the top and the bottom of the sediment column due to the presence of basement fluid flow, which promotes bacterial sulfate reduction below the sulfate minimum zone at elevated temperatures. Pore fluid $\delta^{34}S$ data show the highest values (135 ‰) yet found in the marine environment. The bacterial sulfur isotopic fractionation factor, α, is severely underestimated if the pore fluids of anoxic marine sediments are assumed to be closed systems and Rayleigh fractionation plots yield erroneous values for α by as much as 15‰ in diffusive and advective pore fluid regimes. Model results are consistent with $\alpha = 1.077 \pm 0.007$ with no temperature effect over the range 1.8 to 62°C and no effect of sulfate reduction rate over the range 2 to 10 pmol cm^{-3} d^{-1}. The reason for this large isotopic fractionation is unknown, but one difference with previous studies is the very low sulfate reduction rates recorded, about two orders of magnitude lower than literature values that are in the range of μmol cm^{-3} d^{-1} to tens of nmol cm^{-3} d^{-1}. In general, the greatest ^{34}S depletions are associated with the lowest sulfate reduction rates and vice versa, and it is possible that such extreme fractionation is a characteristic of open systems with low sulfate reduction rates.

1. INTRODUCTION

Bacterial sulfate reduction is an important geological process. Heterotrophic sulfate reduction by obligate anaerobes preferentially utilizes the lighter sulfur isotope ^{32}S, leaving pore fluids progressively enriched in ^{34}S. Sulfate reduced to sulfide by this process reacts with iron to form Fe sulfides and ultimately pyrite (Berner, 1970). The fractionation factor, $\alpha_{SO4\text{-}H2S}$, for bacterial sulfate reduction has been determined through experimental culture studies as $\epsilon = 4$ to 46 ‰ ($\epsilon = 10^3 \ln \alpha$), with an average of 14.3‰ (Böttcher et al., 1999b). However, measured ^{34}S depletions in marine sulfides are larger, typically 24 to 71‰, averaging 51‰ (Goldhaber and Kaplan, 1974; Goldhaber and Kaplan, 1980; Canfield and Teske, 1996; Böttcher et al., 1998; Böttcher et al., 1999a), an effect that is thought to be due to repeated cycles of sulfide oxidation followed by disproportionation in natural systems (Jørgensen, 1990; Canfield and Thamdrup, 1994; Canfield and Teske, 1996; Cypionka et al., 1998).

It was originally thought that the rate of sulfate reduction may play a role in determining the sulfur isotopic fractionation in natural systems (Goldhaber and Kaplan, 1975), but this relationship has been questioned because it requires constant population densities of sulfate-reducing bacteria (Chambers and Trudinger, 1978). A recent compilation of sulfide depletions vs. sulfate reduction rates measured using radiotracers in marine sediments provides no support for the effect of absolute sulfate reduction rate (mass $volume^{-1}$ $time^{-1}$) (Canfield and Thamdrup, 1994; Canfield and Teske, 1996). Rather, the fractionation factor is believed to be influenced by the specific rate of sulfate reduction (mass $cell^{-1}$ $time^{-1}$) (Kaplan and Rittenberg, 1964; Chambers et al., 1975). Habicht and Canfield (1997) noted that other factors, such as sulfate concentration, temperature, pH, bacterial species and growth conditions, may all play a role in determining the isotopic fractionation.

In closed systems, the isotopic fractionation factor may be obtained from direct measurements of the isotopic difference between sulfate and sulfide, assuming Rayleigh-type fractionation (Goldhaber and Kaplan, 1974). However, diagenetic modeling of the sulfate distributions in coastal marine sediments has shown that such sediments are open with respect to sulfate (Jørgensen, 1979). Under these circumstances, Rayleigh fractionation model calculations will underestimate the natural sulfur isotopic fractionation factor.

In this article we consider the bacterial fractionation of sulfur isotopes in anoxic terrigenous clastic sediments. Pore fluid $\delta^{34}S$ data have been measured at four sites drilled to basement on the eastern flank of the Juan de Fuca Ridge, 48° N, during ODP Leg 168 (Davis et al., 1997). The sites all show a middepth sulfate minimum, and at two sites sulfate is fully depleted. However, the presence of basement fluid flow at elevated temperatures (15–62°C) (Davis et al., 1997; Elderfield et al., 1999) provides a supply of sulfate to the base of the sediment column that promotes bacterial sulfate reduction at elevated temperatures (Rudnicki et al., 2000). For comparison with numerical diagenesis modeling of anaerobic bacterial sulfate reduction and isotopic fractionation, we calculate the closed system (Rayleigh) sulfur isotopic fractionation factors and show how diffusion and pore fluid advection can influence these results. A numerical diagenesis model of anaerobic bacterial sulfate reduction is developed to constrain the bacterial isotopic fractionation factor and assess whether there is a

*Author to whom correspondence should be addressed.
†*Present address:* Division of Earth and Ocean Sciences, Duke University, 103 Old Chemistry Building, Durham, NC 27708, USA.

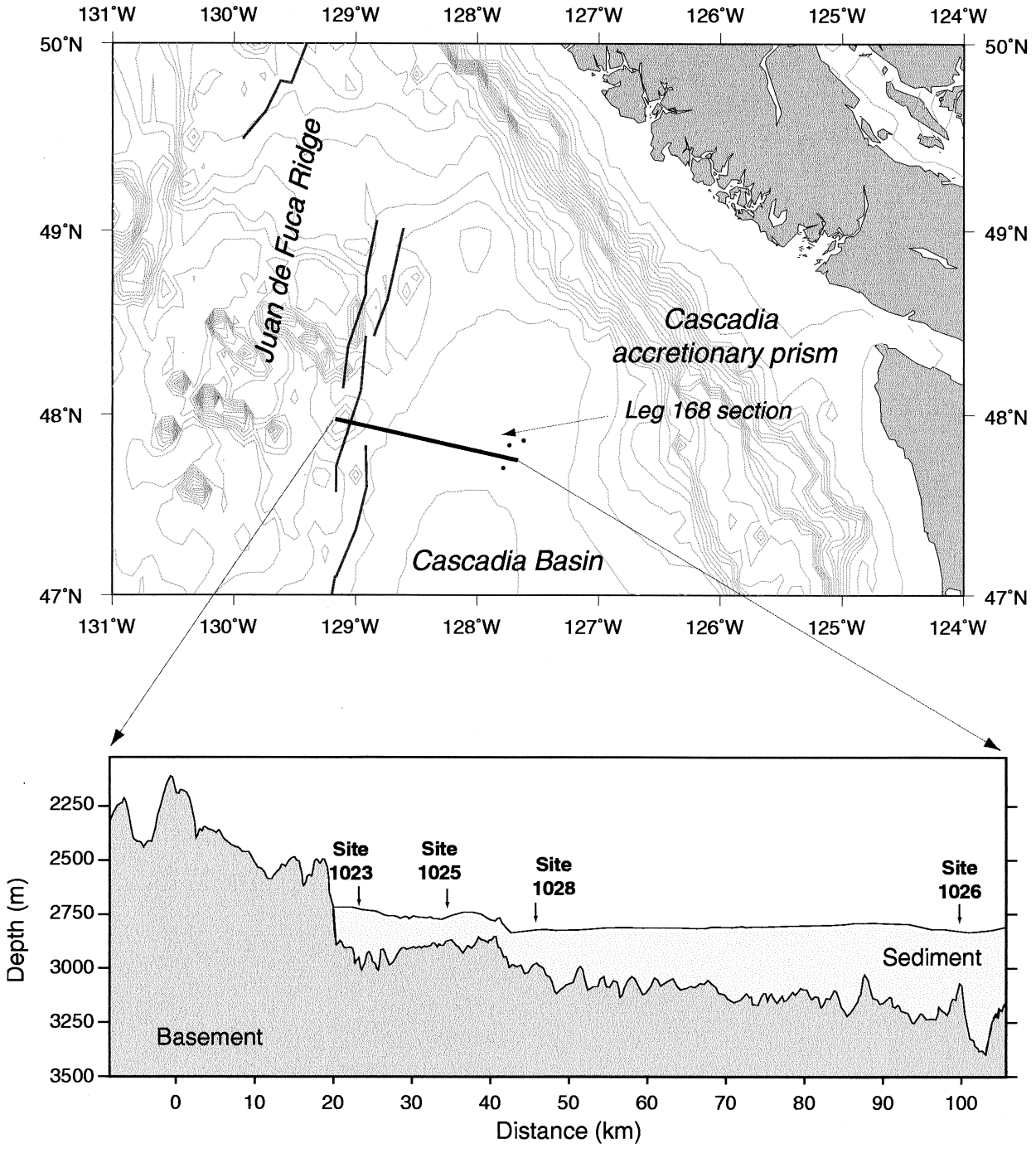

Fig. 1. Location map of the sites considered in this study.

temperature effect on sulfur isotopic fractionation during extremely slow, long-term (<3 Ma) diagenesis.

2. THE EASTERN FLANK OF THE JUAN DE FUCA RIDGE

The eastern flank of the Juan de Fuca Ridge (Fig. 1) has been studied as an area of anomalous heat flow since 1988 (Davis et al., 1989; Davis et al., 1992; Wheat and Mottl, 1994; Thomson et al., 1995; Davis et al., 1997). After drilling during ODP Leg 168, it is now known that the sediment column is underlain by an aquifer carrying fluids of near-seawater composition, of relatively young age (<10 ka) and of increasing temperature away from the ridge axis (Elderfield et al., 1999). Basement temperatures and core details for the four sites studied here are given in Table 1. The morphology of the eastern flank is characterized by a series of axis-parallel basement ridges that outcrop (new data—several more outcrops discovered in 2000) through a thick sequence of Pleistocene turbidites derived from

Table 1. ODP site information for sediments and basement of the east flank of the Juan de Fuca Ridge.

ODP site	1023	1025	1026	1028
Latitude N	47°55.0′	47°53.2′	47°45.8′	47°51.5′
Longitude W	128°47.5′	128°39.0′	127°45.5′	128°22.6′
Basement age (Ma)	0.86	1.24	3.51	1.95
Sediment thickness (m)	192.8	97.5	228.9	220.1
Basement temperature (°C)[a]	15.5	38.6	61.7	58.7
Advective velocity (m Ma^{-1})[b]	−910	95	130	290
Initial carbon, G_0 (mmol kg^{-1})	280	200	190	260

[a] Bottom water temperature is 1.8°C (Davis et al., 1997).
[b] Darcy velocity ($v = \phi v$). Positive velocity signifies upwards advection. Data from Rudnicki et al. (submitted).

the Pacific Northwest. The sediments covering the ridge flanks are hemipelagic and carbonate-rich muds interlayered with turbidite sands and silty sands. The muds are composed of ≈40 wt.% clays, ≈30 wt.% feldspars, and ≈25 wt.% quartz, with ≈5 wt.% pyrite and <5 wt.% carbonate, whereas the turbidites have less clays (≈20 wt.%) and more feldspar (≈50 wt.%) (Davis et al., 1997).

3. METHODS

3.1. Sulfur Isotopic Analysis

Pore fluids were sampled from sediment cores by conventional ODP techniques. The pore fluid samples were expelled from the squeezed sediment into a syringe after all the air had been purged from the interconnecting tubing ensuring anoxic sampling. The samples were analyzed onboard for major elements and nutrients (Davis et al., 1997). Great care was also taken to obtain good data for porosity, formation factor, and temperature down core, to aid the modeling work (Shipboard Scientific Party, 1997). Samples in the form of $BaSO_4$ precipitates were prepared for sulfur isotope analysis according to the method of Coleman and Moore (1978). Where necessary, pore fluid samples were combined (see Table 2) so that the minimum amount of $BaSO_4$ prepared was 2.5 mg. Analysis of SO_2 gas was performed in a VG SIRA 10 mass spectrometer. The isotopic composition of sulfur in a sample is denoted by the permil deviation of the $^{34}S/^{32}S$ isotopic ratio referenced to that of Vienna-Canyon Diabolo troilite (V-CDT):

$$\delta^{34}S = \left[\frac{(^{34}S/^{32}S)_{sample}}{(^{34}S/^{32}S)_{V\text{-}CDT}} - 1 \right] * 1000‰ \quad (1)$$

Reference material IAEA-S-1 (= −0.3 ‰) was used to calibrate the mass spectrometer and NBS 122 gave +0.15 ‰. The overall analytical reproducibility is ±0.15 ‰. Sulfate and $\delta^{34}S$ data are given in Table 2 and plotted in Figure 2a–d.

3.2. Diagenetic Modeling

3.2.1. Closed system (Rayleigh) fractionation

The pore fluids measured in this study record the largest sulfur isotopic fractionations measured in the marine realm—a maximum of $\delta^{34}S$ = 135‰ at site 1028, exceeding the previously reported maximum value of +110‰ (ODP Site 963; Böttcher et al. (1998)) by >20‰. Isotope mixing plots and Rayleigh fractionation plots for each of the four sites are shown in Figure 3a–h. For each site, data above and below the sulfate minimum have been considered separately.

If simple binary mixing is present between two end member fluids of differing $\delta^{34}S$ isotopic composition and sulfate concentration, then an isotope mixing plot of $\delta^{34}S$ vs. $1/SO_4^{2-}$ should show a straight line. Mixing plots for the top of the sections at all sites are either curved (site 1023) or generally irregular (e.g., site 1025), which can arise if there is bacterial sulfate reduction throughout the sediment column. The plots for the bottom of the sections are straighter, reflecting lower sulfate reduction rates below the sulfate minimum. At sites 1023 and 1026 there is clearly removal of sulfate in the basal portion of the sediment column below the broad sulfate minimum, because this is required to maintain the pore fluid gradients. These plots, therefore, show that the sulfate concentrations and isotopic composition are not controlled solely by mixing between fluids at either the upper and lower sediment boundaries, and with the fluids generated at the sulfate minimum.

The isotopic fractionation factors for each site have been calculated by the method of Goldhaber and Kaplan (1974). The relevant Rayleigh equation is given by:

$$R^T_{SO4} = R^0_{SO4} F^{1-(K_2/K_1)} \quad (2)$$

where: K_1 = unidirectional rate constant for $^{32}SO_4$ reduction
K_2 = unidirectional rate constant for $^{34}SO_4$ reduction
R^T_{SO4} = ($^{32}S/^{34}S$) at time T
R^0_{SO4} = ($^{32}S/^{34}S$) at start
$F = [SO_4]_T/[SO_4]_o = C_T/C_0$
Taking logs, and substituting $\alpha = K_1/K_2$, $F = C_T/C_0$, gives:

$$\log R^T_{SO4} = \left(1 - \frac{1}{\alpha}\right) \log C_T + \left[\log R^0_{SO4} - \left(1 - \frac{1}{\alpha}\right) \log C_0 \right] \quad (3)$$

Therefore, the gradient of a plot of $\log(^{32}S/^{34}S)$ vs. $\log(SO_4^{2-})$ is equivalent to $1\text{-}\alpha^{-1}$, where α is the fractionation factor. The fractionation factors, given in Table 3, fall in the range 1.010≈1.061. The average value, 1.046 ± 0.010, excluding the low value calculated for the base of site 1023, is similar to the average for isotopic fractionation measured in natural systems, = 1.051 ± 10‰ (Canfield and Teske, 1996; Böttcher et al., 1999b). However, the isotopic fractionation factor calculated in this way will be underestimated if there is diffusive or advective supply of sulfate to the sulfate reduction system (Jørgensen, 1979; Chanton et al., 1987).

3.2.2. Open system fractionation

The pore water sulfate model of Berner (1978) is based on the microbially mediated reduction of sulfate during organic matter degradation, a reaction that may be summarized as:

$$2CH_2O + SO_4^{2-} \leftrightarrow H_2S + 2\ HCO_3^- \quad (4)$$

The rate law for such a reaction has been found to be approximately dependent on the square of the sedimentation rate (ω) (Toth and Lerman, 1977; Berner, 1978; Tromp et al., 1995):

$$k = 0.057\ \omega^{1.94} \quad (5)$$

where k is in a^{-1}, ω is in cm a^{-1}. This formulation for k is independent of temperature. A recent compilation of sulfate reduction rate vs. temperature (Canfield et al., 2000) has not suggested a temperature effect. This may be a property of mixed populations of sulfate reducers with different temperature adaptations. However, individual species show higher specific rates of metabolism above the optimal growth temperature, with a 10°C increase in temperature causing an increase in metabolic rate of 2 ≈ 4 times (Westrich and Berner, 1988).

The application of this model was previously described (Richter, 1996; Rudnicki et al., 2000), but the outline of the model is reproduced

Table 2. Pore fluid data.

Leg, site	Sample	Depth (mbsf)	Sulfate (mmol kg^{-1})	$\delta^{34}S$ (‰)
168, 1023A	1H-1, 140–150	1.45	25.7	23.7
	1H-2, 140–150	2.95	24.7	22.1
	1H-3, 140–150	4.45	22.7	28.6
	1H-4, 140–150	5.95	22.1	
	1H-5, 140–150	7.45	19.6	
	2H-1, 140–150	10.75	14.2	46.0
	2H-5, 140–150	16.75	9.30	66.7
	3H-5, 140–150	26.25	5.76	87.4
	4H-5, 140–150	35.75	2.02	
	5H-5, 140–150	45.25	0.91	
	6H-5, 140–150	54.75	0.27	
	7H-5, 140–150	64.25	0.00	
	8H-5, 140–150	73.75	0.10	
	9H-5, 140–150	82.85	0.54	
	10H-5, 140–150	92.75	0.44	
	11H-5, 140–150	102.25	0.16	
	12H-5, 140–150	111.75	1.14	
	13H-5, 140–150	121.25	0.38	
	14H-4, 140–150	129.25	0.15	
169, 1023B	15X-2, 135–150	132.93	1.38	
	16X-3, 135–150	137.13	1.32	
	17X-3, 135–150	146.73	0.85	
	18X-4, 135-150	157.83	4.62	
	Mean of 15X-2 ~ 18X-4	143.6 ± 12.5 m	[2.04]	[28.5]
	19X-2, 135–150	164.53	7.58	34.4
	20X-4, 135–150	177.13	13.4	27.1
	21X-3, 135–150	185.23	19.7	24.4
	21X-4, 135–150	186.73	20.8	24.2
	21X-5, 110–125	187.98	21.5	22.6
	21X-6, 75–85	189.10	22.9	21.8
	22X-1, 88–103	191.36	23.8	
	22X-2, 47–62	191.98	24.2	22.8
168, 1025A	1H-1, 140–150	1.45	26.9	23.7
	1H-3, 140–150	4.45	20.7	31.9
168, 1025B	1H-2, 140–150	2.95	23.3	25.9
	2H-1, 140–150	6.45	15.7	43.1
	2H-2, 140–150	7.95	14.4	
	2H-3, 140–150	9.45	13.8	58.5
	2H-4, 140–150	10.95	12.9	62.0
	3H-5, 140–150	21.95	8.52	
	4H-5, 140–150	31.45	12.2	68.8
	5H-5, 140–150	40.95	13.7	59.7
	6H-5, 140–150	50.45	16.8	50.8
	7H-5, 140–150	59.95	20.0	36.2
	8H-5, 140–150	69.45	21.8	
	10X-1, 135–150	82.53	26.8	24.1
	10X-5, 135–150	88.53	26.1	
	11X-2, 135–150	93.63	26.0	19.8
	11X-3, 135–150	95.13	27.3	
	11X-4, 135–150	96.63	26.7	21.7
168, 1026A	1H-1, 140–150	1.45	25.7	23.8
	1H-2, 140–150	2.95	25.7	
	1H-3, 140–150	4.45	22.9	29.2
	2H-2, 140–150	8.35	15.2	
	2H-3, 140–150	9.85	13.8	53.1
	2H-5, 140–150	12.85	12.1	52.6
	3H-5, 140–150	22.35	7.30	
	4H-3, 140–150	28.85	4.01	
	Mean of 3H-5 ~ 4H-3	27.1 ± 5 m	[5.7]	[100.3]
	4H-5, 140–150	31.85	4.21	
	5H-5, 140–150	41.35	0.33	
	6H-1, 140–150	44.85	0.85	
	6H-2, 60–70	45.55	0.49	
	7H-5, 140–150	60.35	0.31	
	8H-6, 130–140	71.25	0.55	
	8H-6, 140–150	71.35	0.11	
	9H-4, 140–150	77.85	1.76	
	10H-3, 110–120	85.55	0.55	
	10H-5, 140–150	88.85	1.08	
	11H-5, 140–150	98.35	1.57	
168, 1026C	4R-1, 45–128	114.71	0.89	
	5R-1, 135–150	124.53	0.68	
	7R-1, 128–148	143.68	3.46	
	8R-1, 63–78	152.71	3.88	
	9R-1, 135–150	163.03	5.56	
	Mean of 8R-1 ~ 9R-1	157.9 ± 5 m	[4.72]	[70.3]
	10R-2, 135–150	174.13	9.18	
	10R-5, 135–150	178.63	10.1	
	12R-1, 130–150	191.90	11.8	
	13R-4, 130–150	206.00	13.9	29.6
	14R-4, 130–150	215.60	13.9	
	15R-1, 81–104	220.23	14.1	29.7
	15R-2, 66–86	221.56	14.8	
	15R-3, 59–79	222.99	14.6	28.1
	15R-4, 130–150	225.20	14.1	
	15R-5, 45–65	225.85	14.8	27.2
	15R-6, 70–90	227.60	15.1	30.4
	15R-7, 25–45	228.65	14.4	
168, 1028A	1H-1, 140–150	1.45	25.9	22.8
	1H-2, 140–150	2.95	23.7	25.9
	2H-3, 140–150	8.25	13.5	
	3H-2, 140–150	16.15	5.33	84.6
	4H-5, 140–150	30.15	2.55	
	5H-5, 140–150	39.65	2.71	
	6H-5, 140–150	49.15	3.01	
	Mean of 4H-5 ~ 6H-5	39.7 ± 10 m	[2.76]	[135.2]
	7H-5, 140–150	58.65	3.39	
	8H-5, 140–150	68.15	3.94	
	Mean of 7H-5 ~ 8H-5	63.4 ± 5 m	[3.67]	[102.0]
	9H-5, 135–150	77.63	5.96	79.9
	10H-5, 135–150	87.13	7.93	58.8
	11H-5, 135–150	96.63	9.22	53.6
	12H-5, 135–150	106.13	10.5	46.3
	13X-2, 135–150	111.13	12.1	40.6
	13X-5, 135–150	115.50	12.3	40.5
	15X-1, 135–150	125.23	13.9	32.9
	15X-2, 135–150	126.73	14.2	34.7
	15X-3, 135–150	128.23	14.1	33.1
	15X-4, 135–150	129.73	14.7	33.6
	15X-6, 0–15	131.38	15.0	31.2

here for convenience. The diagenetic model described by Richter and DePaolo (1987) provides a useful framework for assessing pore fluid advection, diffusion and reaction in an evolving sediment column.

The standard 1-dimensional diagenetic equation (Berner, 1980) is given by:

$$\frac{\partial \phi C}{\partial t} = \frac{\partial}{\partial z}\left(\phi D_c \frac{\partial C}{\partial z}\right) - \frac{\partial \phi v C}{\partial z} + \phi \Sigma R \qquad (6)$$

where C represents the concentration of a solute, ϕ is the porosity, t = time, z = height above basement, D_C is the diffusivity relevant for the solute C, v is the advective velocity, and ΣR represents the sum of the reaction terms. D_C is corrected for tortuosity by using the relationship $D_C = D^0/\phi f$, where D^0 is the coefficient of diffusion at infinite dilution and f is the formation factor (McDuff and Ellis, 1979). The product ϕv (hereafter denoted by v) is the Darcy velocity. The diffusion rate is

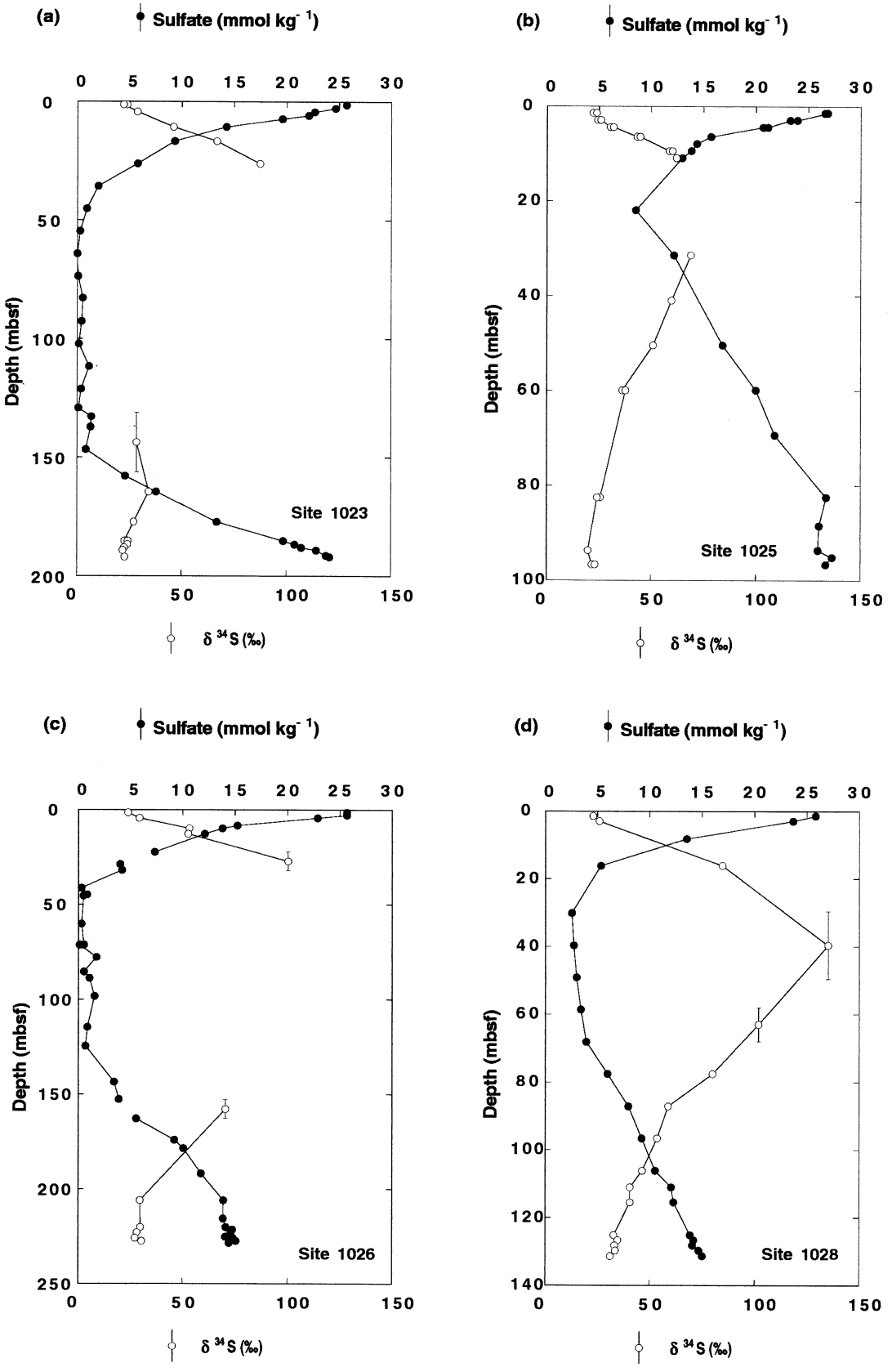

Fig. 2. (a–d) Measured sulfate and $\delta^{34}S$ data for (a) site 1023, (b) site 1025, (c) site 1026, and (d) site 1028. The depth range is given where combined samples have been analyzed for $\delta^{34}S$.

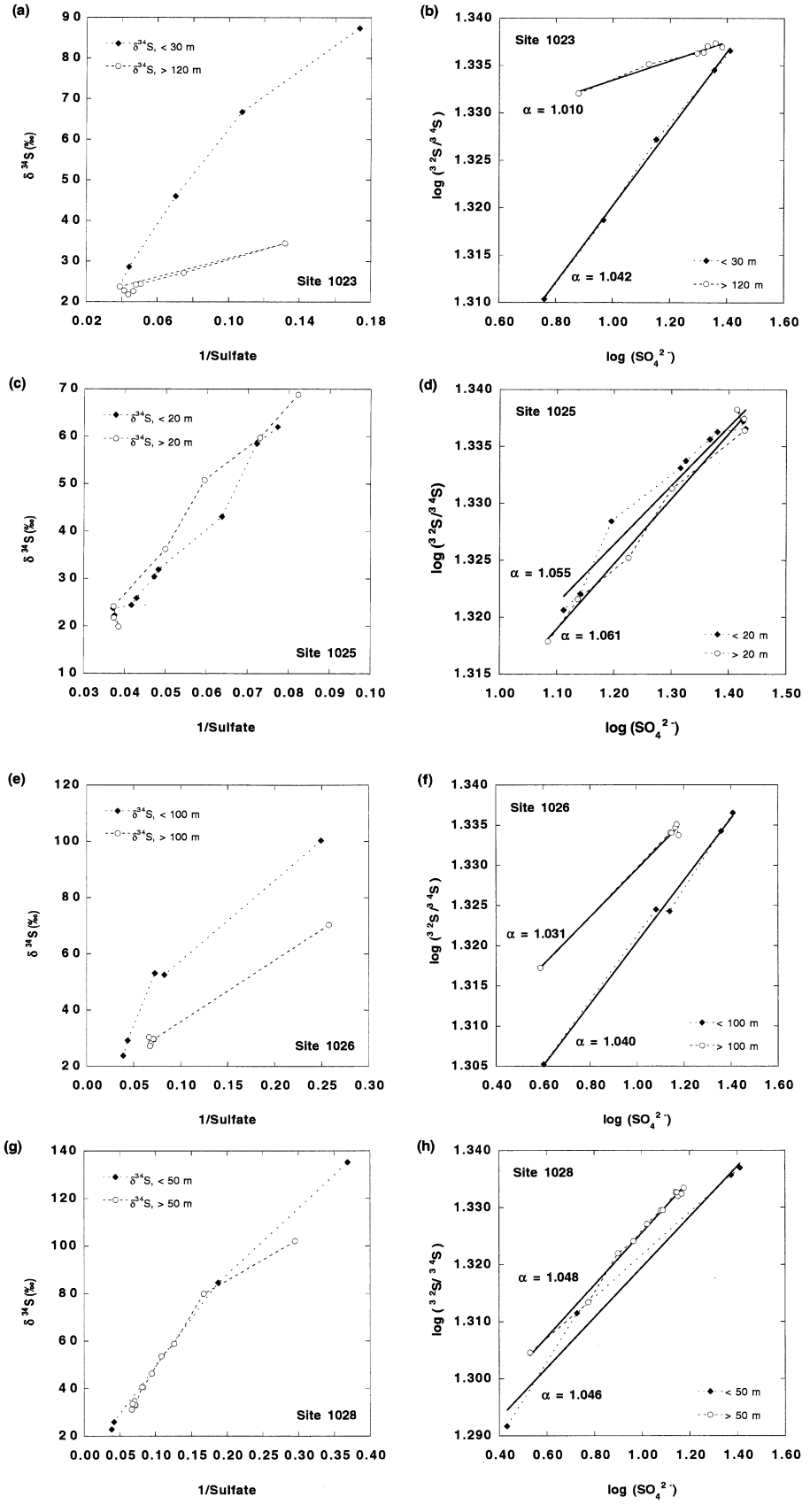

Fig. 3. (a–h) Isotope mixing plots and Rayleigh plots for (a,b) site 1023, (c,d) site 1025, (e,f) site 1026, and (g,h) site 1028.

Table 3. Rayleigh sulfur isotopic fractionation $\alpha_{SO4-H2S}$ results.

Site	Above sulfate minimum	Below sulfate minimum
Site 1023	1.042 ± 0.001	1.010 ± 0.001
Site 1025	1.055 ± 0.005	1.061 ± 0.003
Site 1026	1.040 ± 0.002	1.031 ± 0.001
Site 1028	1.046 ± 0.005	1.048 ± 0.001

related to the temperature, porosity, and tortuosity of the sediment, parameters that vary with depth, such that the complete diffusive flux term is given by (Berner, 1980):

$$\frac{\partial}{\partial z}\left(\phi D_c \frac{\partial C}{\partial z}\right) = \phi\left(D_c \frac{\partial^2 C}{\partial z^2} + \left(\frac{\partial D_c}{\partial z^2} + \frac{D_c}{\phi}\frac{\partial \phi}{\partial z}\right)\frac{\partial C}{\partial z}\right) \quad (7)$$

Provided that temperature, porosity, and formation factor can be expressed as simple analytical functions vs. depth, then the gradient terms involving diffusion and porosity can be readily evaluated. Temperature and porosity vs. depth for each of the Leg 168 sites are given in Davis et al. (1997).

In the Richter and DePaolo formulation, time-dependent porosity is taken into account when layers of sediment are deposited in the model. This results in sediment compaction and pore fluid expulsion. Between layer deposition, Eqn. 6 and Eqn. 7 are combined to give the final form of the conservation equation:

$$\frac{\partial C}{\partial t} = D_c \frac{\partial^2 C}{\partial z^2} + \left(\frac{\partial D_c}{\partial z} + \frac{D_c}{\phi}\frac{\partial \phi}{\partial z} - \frac{v}{\phi}\right)\frac{\partial C}{\partial z} + \Sigma R \quad (8)$$

Lasaga (1979) has shown that electrical effects due to the conservation of electroneutrality in marine pore fluids are unimportant for all ions other than Cl^- and Na^+. This view has recently been reiterated by Boudreau (1997). However, diffusive flux coupling, whereby the strong gradients of one species may lead to a flux of another is an important effect that has not been routinely considered for marine pore fluids, although it is common for models of diffusion in silicate melts (Liang et al., 1996a; Liang et al., 1996b; Liang et al., 1997). In pore fluids, strong sulfate gradients lead to fluxes of magnesium and calcium, although the effect on sulfate concentrations is minor and can be ignored (Lasaga, 1981; Applin and Lasaga, 1984; Felmy and Weare, 1991b; Felmy and Weare, 1991a).

The model run proceeds as follows. First, the sediment is decompacted according to the porosity-depth relationship and divided into sections of thickness Δz. We set $\Delta z = 2$ m for all sites. The sediment slices are deposited at the appropriate time during the model run. With each new layer, the sediment pile is compacted, resulting in pore water advection due to loss of porosity. Until the next layer is required, the model is stepped in time allowing for advection, diffusion, and reaction. We solve Eqn. 8 by using the DuFort–Frankel scheme, an explicit, three-level finite difference method that uses differences centered both in time and space (DuFort and Frankel, 1953; Hoffman, 1992). See Richter and DePaolo (1987) for further details of the method of solution. These processes are continued until the model time reaches the present day.

The conservation equation for sulfate is derived by setting $C = [SO_4^{2-}]$ and specifying the reaction term as:

$$\Sigma R_{SO4} = -\frac{\rho_s(1-\phi)}{\rho_f \phi} Lk \left[\frac{[SO_4^{2-}]}{K_{SO4} + [SO_4^{2-}]}\right][G] \quad (9)$$

where ρ_s and ρ_f are the sediment and fluid densities, L (=0.5) is a stoichiometric constant representing the ratio of sulfate to organic matter consumed in Eqn. 4, and G = organic carbon concentration. The D^0 value for sulfate (Boudreau, 1997) is given by: $D_0^{SO4} = (4.88 + 0.232\ T) * 10^{-6}\ cm^2 s^{-1}$, where T = temperature in °C. The rate of organic matter degradation is controlled by using Monod kinetics, where K_{SO4} is the saturation constant (Monod, 1949). We set $K_{SO4} = 1$ mmol kg^{-1}. When $[SO_4^{2-}] \gg K_{SO4}$, the rate of organic matter degradation is independent of the sulfate ion concentration but becomes first order in sulfate when $[SO_4^{2-}] \ll K_{SO4}$. This prevents negative sulfate concentrations that can occur in the Berner model if the oxidant (sulfate) is exhausted before all the organic matter is oxidized (Boudreau and Westrich, 1984).

$\delta^{34}S$ is calculated as $\delta^{34}S^*$ (i.e., $(1 + \delta^{34}S/1000) * [SO_4^{2-}]$), following the $\delta^{14}C^*$ notation of Craig (1969), such that the reaction term is given by:

$$\Sigma R_{\delta 34S^*} = \frac{1}{\alpha_{SO_4-H_2S}} \frac{[\delta^{34}S^*]}{[SO_4^{2-}]} \Sigma R_{SO4} \quad (10)$$

We run the model to obtain the best least-squares fit for α.

4. RESULTS

The effects of varying degrees of "openness" on closed system calculations of the sulfur isotope fractionation factor can be examined by considering the effects of diffusion and advection in a model sediment column. We have calculated model curves for sulfate and $\delta^{34}S$ for site 1025 by the method described in Section 3.2.2, based on a range of constant values for α, considering the cases in which diffusion and advection are both present or absent. For each scenario, we obtain a plot of the calculated closed system (Rayleigh) value for α vs. the model value (Fig. 4a,b). For the case of no diffusion and advection, the calculated values for α are within 0.5‰ of the model values for fractionation factors up to $\alpha = 1.100$. This slight discrepancy arises because the model sediment is not entirely free of advection; there is some fluid movement due to loss of porosity and also due to pore fluid burial. If, however, diffusion is allowed in the model, then the calculated α will significantly underestimate the actual model fractionation factor, e.g., by 15‰ for a model fractionation of 70‰. Adding an upward advective flow of 200 m Ma^{-1}, typical for the sediments in this study, increases the discrepancy, although the effect is minor for a diffusive regime. In conclusion, any violation of the assumption of a closed geochemical system, either through advection or diffusion, will result in an underestimation of the sulfur isotope fractionation factor if a Rayleigh model is used.

Sulfate and $\delta^{34}S$ model results for the four sites considered in this study are presented in Figure 5a–d. Sulfate profiles were previously modeled by Rudnicki et al. (2000), and their data for the initial carbon (G_0) content of the solid and the rate of pore fluid advection are given in Table 1. Model sulfate curves provide a good fit to the data for sites 1025 and 1028, but the profiles for sites 1023 and 1026 below the sulfate minimum zone are not well modeled. This may be due to variations in sediment properties, variations in the initial organic carbon content of the sediment, or may reveal limitations of the Berner sulfate model. For these reasons we do not draw any firm conclusions from these sites alone in the discussion below. Sulfate is fully depleted to <1 mmol kg^{-1} at sites 1023 and 1026, where continued bacterial degradation of organic matter produces methane. The formation of methane and the oxidation of methane via sulfate reduction to form bicarbonate would have implications for the pore fluid concentrations discussed in this article if the rates of bacterial methanogenesis were similar to those for bacterial sulfate reduction. Current estimates are that the rates of methanogenesis are an order of magnitude lower than for sulfate reduction (Tromp et al., 1995), and as such can be excluded from the present model.

Model sulfate reduction rates are shown in Figure 6a,b.

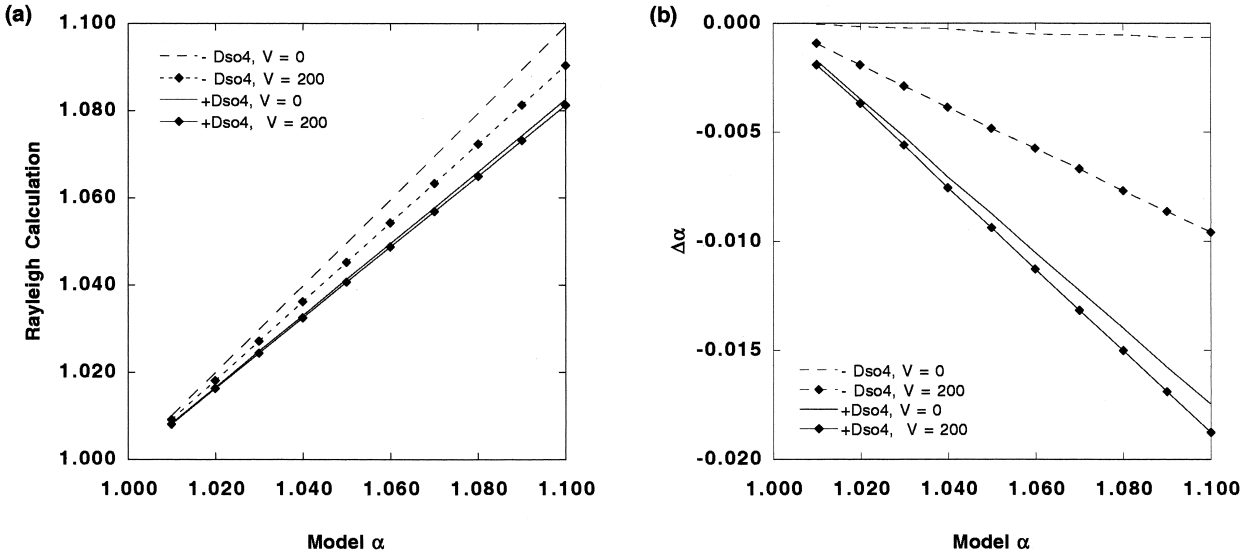

Fig. 4. (a) A comparison between the model fractionation factor α and that calculated assuming closed system Rayleigh fractionation. (b) Difference between the calculated Rayleigh α and model α.

Because the rate of organic matter consumption is a function of the rate of sedimentation, Eqn. 5, this leaves regions of the sediment column where slow long-term sulfate reduction is sustained by the availability of organic matter. These regions exert a control on the pore fluid sulfate and $\delta^{34}S$ profiles that determine the model results. It is important to note that there is sulfate reduction, and thus excess organic carbon, below the sulfate pore fluid minimum at all sites except site 1023.

The best fit α for each site was obtained by minimizing the least squares error between the modeled and measured data. Least squares error plots for α, varying between 1.00 and 1.10, are given in Figure 7. It is not possible to specify a constant value for α to fit the $\delta^{34}S$ profile above and below the sulfate minimum at site 1023. Instead, values for α consistent for the pore fluid data above and below the sulfate minimum are given in Table 4. The model value for α below the sulfate minimum ($\alpha = 1.010$) agrees with the Rayleigh α. This may be an artifact of applying the Rayleigh model to a situation in which there is simple mixing and in which the pore fluid sulfate is not well reproduced by the open system model (Fig. 5a). The constant fractionation factors for sites 1025, 1026, and 1028 are similar ($\bar{\alpha} = 1.077 \pm 0.007$). To determine whether the sulfur isotopic fractionation factor varies in any systematic way downcore, the model has been rerun to fit the $\delta^{34}S$ data below the sulfate minimum. The average value for α obtained for sites 1025, 1026, and 1028 is $\bar{\alpha} = 1.075 \pm 0.005$, indistinguishable from the results detailed above, which are principally determined by sulfate reduction in the upper part of the sediment column. These results, summarized in Figure 8, indicate no downcore variation of α. Therefore, although sulfate reduction persists at these sites and occurs at elevated temperature, we see no evidence for a variation of α with either temperature or sulfate reduction rates within the range of temperatures (1.8–62°C) and reduction rates (2–10 pmol cm^{-2} d^{-1}) seen here.

5. DISCUSSION AND CONCLUSIONS

Open system modeling of bacterial sulfate reduction in the sediments of the Cascadia Basin results in a calculated isotopic fractionation factor of 1.077 ± 0.007. This is the highest sulfur isotopic fractionation observed in the marine realm and results in pore fluid sulfate with measured $\delta^{34}S$ up to 135‰. The extremely low rates of sulfate reduction (<10 pmol cm^{-3} d^{-1}) modeled here means that pore fluid transport (diffusion and advection) is significant in determining the openness of the pore fluid system, and explains the large discrepancy between the calculated Rayleigh values for α and the modeled open system values. As sulfate reduction rates increase, pore fluid transport becomes less important so that, eventually, the setting of sulfate reduction will approximate a closed system. In sediment incubations, Habicht and Canfield (1997) observed the highest sulfur isotopic fractionations (40‰) at low temperatures (15–20°C) and low sulfate reduction rates (<10 μmol cm^{-3} d^{-1}). This range of conditions may be compared with the wider temperature range (1.8–62°C) and extremely slow sulfate reduction rates (2–10 pmol cm^{-3} d^{-1}) at the Leg 168 sites considered here.

Because there is a source of seawater sulfate at the base of the sediment column from off-axis hydrothermal circulation, sulfate reduction in these sediments can be thought of as consisting of two systems, operating above and below the sulfate minimum, at different temperatures. We have tested whether there is a consistent variation of α with temperature by applying an open system model to determine α both above and below the sulfate minimum. There is no systematic variation of α with depth, temperature, or sulfate reduction rate. This is an unexpected result because it would seem likely that variations of α would accompany changes in the organic matter utilised, the products of fermentation, and electron donors. Our data are, therefore, consistent with the findings of Böttcher et al. (1999b) who have concluded, on the basis of laboratory cultures, that the processes responsible for the fractionation of sulfur isotopes

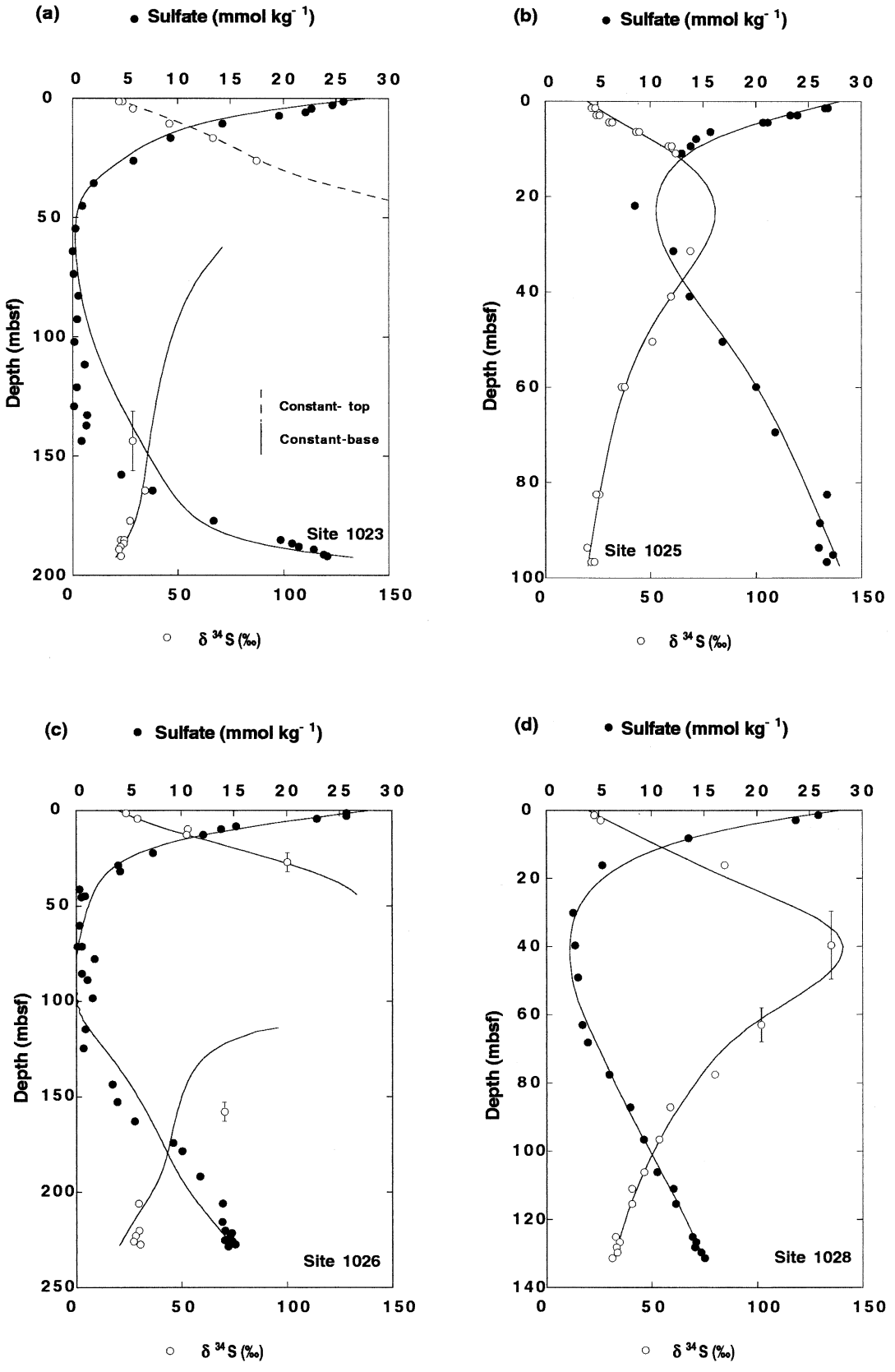

Fig. 5. (a–d) Measured and modeled sulfate and $\delta^{34}S$ data for (a) site 1023, (b) site 1025, (c) site 1026, and (d) site 1028.

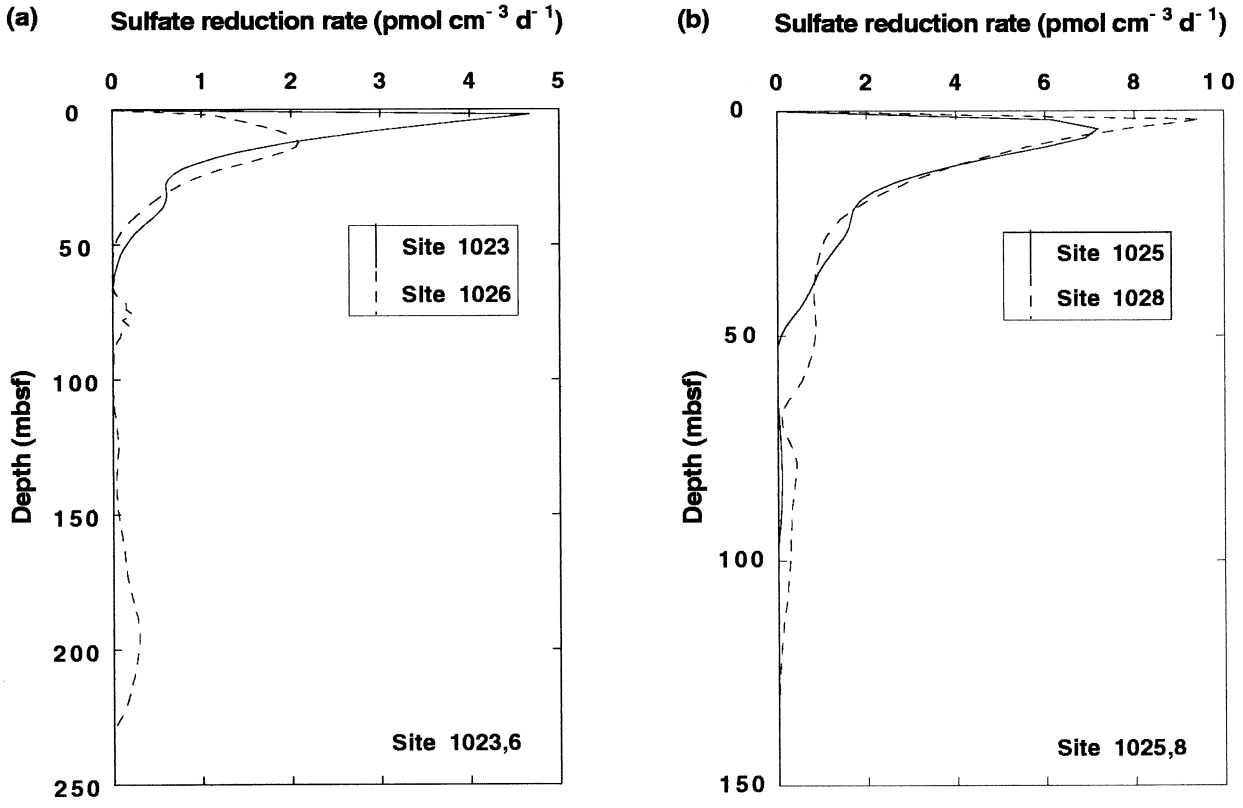

Fig. 6. Calculated model sulfate reduction rates for (a) sites 1023 and 1026 and (b) sites 1025 and 1028.

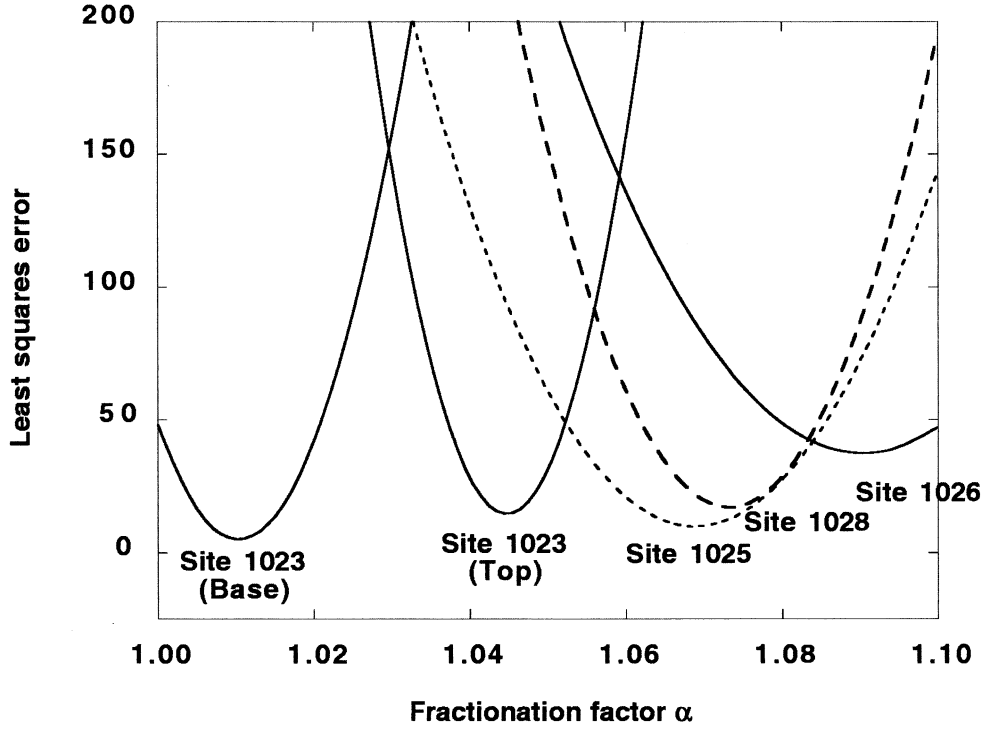

Fig. 7. Least squares ($n^{-1} \Sigma [y_i - y(x_i; \alpha)]^2$; i = 1. . . n) error curves for fitting the bacterial sulfur isotopic fractionation factor, α.

Table 4. Modeled open system sulfur isotopic fractionation $\alpha_{SO4-H2S}$ results.

Site	Above sulfate minimum	Below sulfate minimum
Site 1023	1.048	1.010
Site 1025	1.072	1.070
Site 1026	1.085	1.080
Site 1028	1.073	1.075

in mesophile (<40°C) and thermophile (60°C) bacteria seem to be similar and are associated with comparable isotope fractionations.

What is remarkable about our observations is the very high isotopic fractionation factor of 1.077 ± 0.007. Several studies have recorded large ^{34}S depletions in marine sulfide minerals, equivalent to α up to ≈1.07 (Canfield and Thamdrup, 1994; Canfield and Teske, 1996). However, this is thought to result from repeated cycles of sulfide oxidation and subsequent disproportionation. Therefore, although the sedimentary sulfides may develop extreme ^{34}S depletions, these processes cannot explain the observed extreme enrichments in $\delta^{34}S$ of dissolved sulfate.

An explanation for the extreme $\delta^{34}S$ enrichments measured in pore fluid sulfate at the sites studied here is not clearly evident from previous studies. One obvious issue is sulfate reduction rate. Previous studies have involved systems with sulfate reduction rates of the order of μmol cm^{-3} d^{-1} to tens of nmol cm^{-3} d^{-1}. This compares with rates of the order of pmol cm^{-3} d^{-1} estimated here (Fig. 6). Although no significant correlation has been found between sulfate reduction rate and isotopic fractionation factor, most work shows that the largest ^{34}S depletions during sulfate reduction are associated with the lowest rates of sulfate reduction (Canfield and Teske, 1996; Habicht and Canfield, 1997). This is supported when our data are compared with literature values (Fig. 9). We cannot compare specific rates of sulfate reduction, which Habicht and Canfield (1997) consider to be more important than the absolute rates. A further issue is that sulfate reduction by natural bacterial populations has been found to produce greater isotopic fractionation than in pure cultures with seawater sulfate concentrations (Habicht and Canfield, 1997). This observation has been attributed to lower supply rates of sulfate and use of electron donors other than H_2 in the natural populations. Clearly, it would be very instructive to attempt culture experiments at the low rates estimated at the ODP sites and to examine more deep sea sites. The interpretation of seawater evolution from the S isotopic records of sulfate or sedimentary sulfides (Canfield and Teske, 1996; Paytan et al., 1998) requires

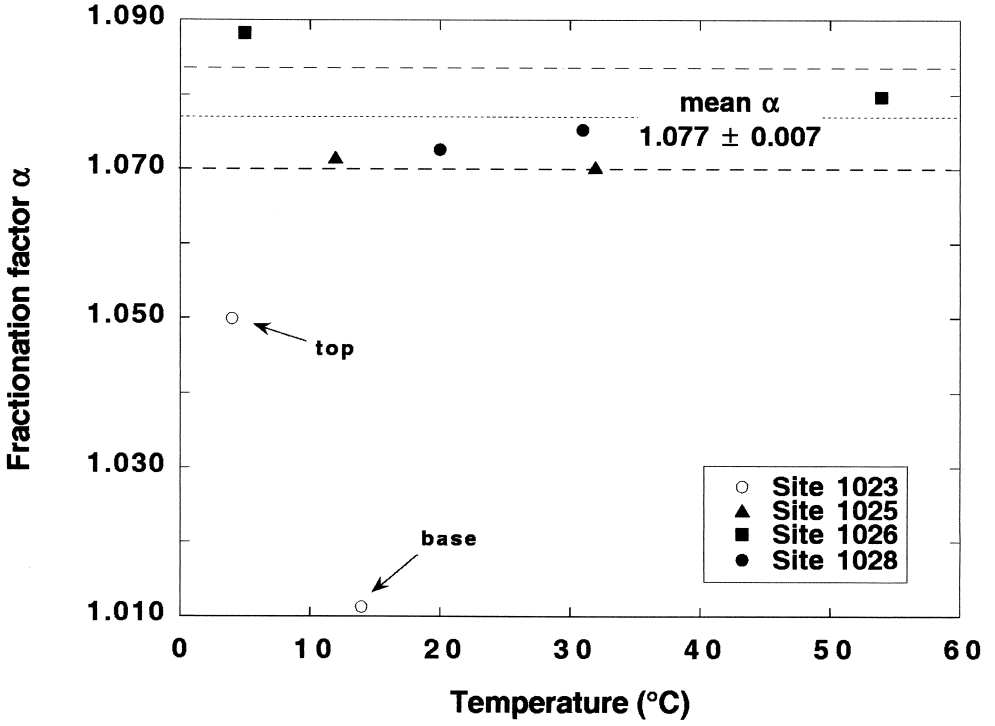

Fig. 8. Compilation of the modeled bacterial $\delta^{34}S$ fractionation factors, determined above and below the sulfate minimum from the Leg 168 sites. The constant α fractionation factors have been plotted at the temperature corresponding to the sulfate reduction rate maximum above and below the sulfate minimum, Fig. 7a,b. These are site 1025, 12°C at 28 m and 32°C at 80 m; site 1026, 5°C at 13 m and 54°C at 200 m; site 1028, 20°C at 50 m and 31°C at 80 m. For site 1023, the constant α for the top of the sediment column has been plotted at 4°C corresponding to a depth of 37 m. The model indicates no sulfate reduction below 50 m, so the bottom value for α is unconstrained. Here, it has been plotted at 14°C, the temperature at the base of the sediment column. The temperature vs. depth relationships are site 1023: $T = 1.80 + 0.071\ d$; site 1025: $T = 1.79 + 0.377\ d$; site 1026: $T = 1.81 + 0.261\ d$; site 1028: $T = 1.80 + 0.367\ d$, where d = depth in mbsf.

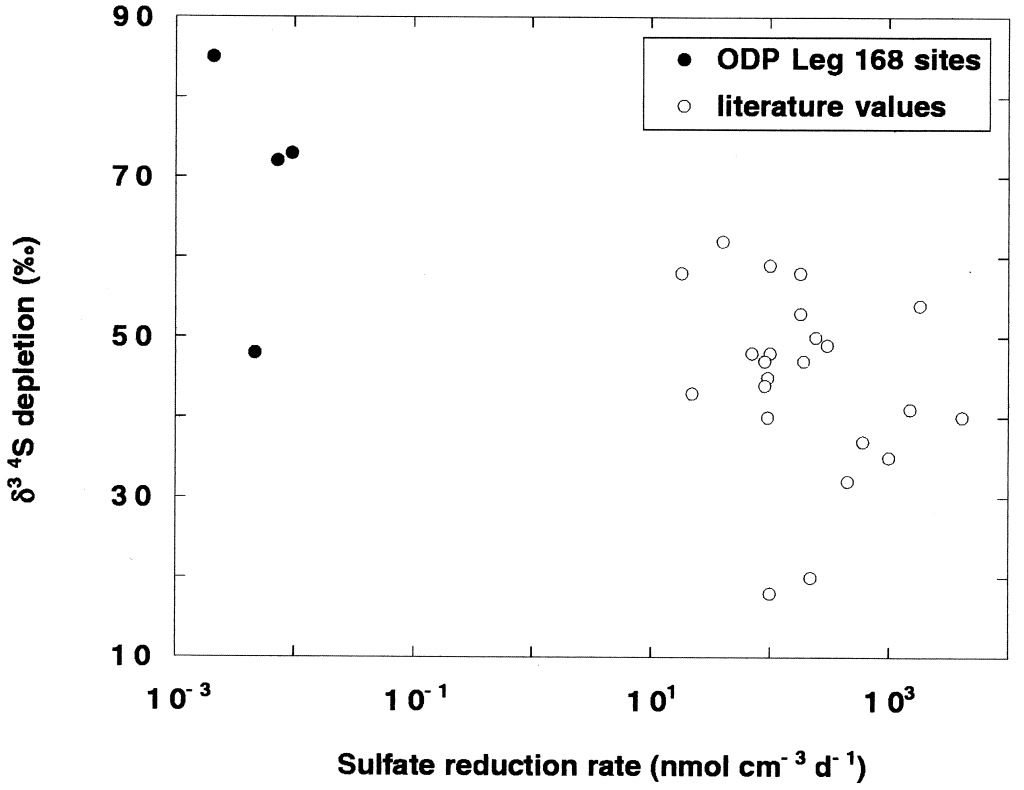

Fig. 9. Comparison of the sulfur isotopic fractionations recorded from the Leg 168 sites compared with literature values, plotted against the sulfate reduction rate. Literature values are from Canfield and Teske (1996).

an understanding of the wider range in the isotopic fractionation of seawater sulfate now recognized.

Acknowledgments—We thank the shipboard personnel of the JOIDES Resolution during Leg 168. M. E. Böttcher (Max-Planck Institute, Bremen) is thanked for reviewing an early draft of this work and for pointing out post-1970s sulfur isotopic fractionation literature. We thank Robert Berner and an anonymous reviewer for their comments. This research was supported by NERC grants GR3/R9705 and GST/02/2025 (H.E.) and a Leverhulme research grant to M.D.R. This is Cambridge Earth Sciences contribution number 6092.

Associate editor: H. Ohmoto

REFERENCES

Applin K. R. and Lasaga A. C. (1984) The determination of SO_4^{2-}, $NaSO_4^-$, and $MgSO_4^0$ tracer diffusion coefficients and their application to diagenetic flux calculations. *Geochim. Cosmochim. Acta* **48,** 2151–2162.

Berner R. A. (1970) Sedimentary pyrite formation. *Am. J. Sci.* **268,** 1–12.

Berner R. A. (1978) Sulfate reduction and the rate of deposition of marine sediments. *Earth Planet. Sci. Lett.* **37,** 492–498.

Berner R. A. (1980) *Early Diagenesis.* Princeton Univ. Press.

Böttcher M. E., Bernasconi S. M., and Brumsack H.-J. (1999a) Carbon, sulfur and oxygen isotope geochemistry of interstitial waters from the western Mediterranean. In *Proc. ODP. Sci. Results* (eds. R. Zahn, M. C. Comas, and A. Klaus), Vol. 161, pp. 413–421. Ocean Drilling Program.

Böttcher M. E., Brumsack H.-J., and de Lange G. J. (1998) Sulfate reduction and related stable isotope (^{34}S, ^{18}O) variations in interstitial waters from the eastern Mediterranean. In *Proc. ODP. Sci. Results* (eds. A. H. F. Robertson, K.-C. Emeis, C. Richter, and A. Camerlenghi), Vol. 160, pp. 365–373. Ocean Drilling Program.

Böttcher M. E., Sievert S. M., and Kuever J. (1999b) Fractionation of sulfur isotopes during dissimilatory reduction of sulfate by a thermophilic gram-negative bacterium at 60°C. *Arch. Microbiol.* **172,** 125–128.

Boudreau B. P. (1997) *Diagenetic Models and Their Implementation.* Springer-Verläg.

Boudreau B. P. and Westrich J. T. (1984) The dependence of bacterial sulfate reduction on sulfate concentration in marine sediments. *Geochim. Cosmochim. Acta* **48,** 2503–2516.

Canfield D. E., Habicht K. S., and Thamdrup B. (2000) The Archean sulfur cycle and the early history of atmospheric oxygen. *Science* **288,** 658–661.

Canfield D. E. and Teske A. (1996) Late Proterozoic rise in atmospheric oxygen concentration inferred from phylogenetic and sulfur isotope studies. *Nature* **382,** 127–132.

Canfield D. E. and Thamdrup B. (1994) The production of ^{34}S-depleted sulfide during bacterial disproportionation of elemental sulfur. *Science* **266,** 1973–1975.

Chambers L. A. and Trudinger P. A. (1978) Microbiological fractionation of stable sulfur isotopes: A review and critique. *Geomicrobiol. J.* **1,** 249–295.

Chambers L. A., Trudinger P. A., Smith J. W., and Burns M. S. (1975) Fractionation of sulfur isotopes by continuous cultures of *Desulfivibrio desulfuricans. Can. J. Microbiol.* **21,** 1602–1607.

Chanton J. P., Martens C. S., and Goldhaber M. B. (1987) Biogeochemical cycling in an organic-rich coastal marine basin. 8. A sulfur isotopic budget balanced by differential diffusion across the sediment-water interface. *Geochim. Cosmochim. Acta* **51,** 1201–1208.

Coleman M. L. and Moore M. P. (1978) Direct reduction of sulfates to sulfur dioxide for isotopic analysis. *Anal. Chem.* **50,** 1594–1595.

Craig H. (1969) Abyssal carbon and radiocarbon in the Pacific. *J. Geophys. Res.* **74,** 5491–5506.

Cypionka H., Smock A. M., and Böttcher M. E. (1998) A combined

pathway of sulfur compound disproportionation in *Desulfovibrio desulfuricans*. *FEMS Microbiol. Lett.* **166,** 181–186.

Davis E. E., Chapman D. S., Forster C. B., and Villinger H. (1989) Heat-flow correlated with basement topography on the Juan de Fuca Ridge flank. *Nature* **342,** 533–537.

Davis E. E., Chapman D. S., Mottl M. J., Bentkowski W. J., Dadey K., Forster C., Harris R., Nagihara S., Rohr K., Wheat G., and Whiticar M. (1992) FlankFlux: An experiment to study the nature of hydrothermal circulation in young oceanic crust. *Can. J. Earth Sci.* **29,** 925–952.

Davis E. E., Fisher A. T., Firth JV, et al. (1997) Hydrothermal circulation in the oceanic crust: Eastern flank of the Juan de Fuca Ridge. *Proc. ODP Initial Reports.* Vol. 168, pp. 1–470. Ocean Drilling Program, College Station.

DuFort E. C. and Frankel S. P. (1953) Stability conditions in the numerical treatment of parabolic differential equations. *Mathematical Tables and Other Aids to Computation* **7,** 135–152.

Elderfield H., Wheat C. G., Mottl M. J., Monnin C., and Spiro B. (1999) Fluid and geochemical transport through oceanic crust: A transect across the flank of the Juan de Fuca Ridge. *Earth Planet. Sci. Lett.* **172,** 151–165.

Felmy A. R. and Weare J. H. (1991a) Calculation of multicomponent ionic diffusion from zero to high concentration. II. Inclusion of associated ion species. *Geochim. Cosmochim. Acta* **55,** 133–144.

Felmy A. R. and Weare J. H. (1991b) Calculation of multicomponent ionic diffusion from zero to high concentrations. 1. The system Na-K-Ca-Mg-Cl-SO_4-H_2O at 25°C. *Geochim. Cosmochim. Acta* **55,** 113–131.

Goldhaber M. B. and Kaplan I. R. (1974) The sulfur cycle. In *The Sea* (ed. E. Goldberg), Vol. 5, pp. 569–655. Wiley.

Goldhaber M. B. and Kaplan I. R. (1975) Controls and consequences of sulfate reduction rates in recent marine sediments. *Soil. Sci.* **119,** 42–55.

Goldhaber M. B. and Kaplan I. R. (1980) Mechanisms of sulfur incorporation and isotopic fractionation during early diagenesis in sediments of the Gulf of California. *Mar. Chem.* **9,** 95–143.

Habicht K. S. and Canfield D. E. (1997) Sulfur isotope fractionation during bacterial sulfate reduction in organic-rich sediments. *Geochim. Cosmochim. Acta* **61,** 5351–5361.

Hoffman J. D. (1992) *Numerical Methods for Engineers and Scientists.* McGraw-Hill, Inc.

Jørgensen B. B. (1979) A theoretical model of the stable sulfur isotope distribution in marine sediments. *Geochim. Cosmochim. Acta* **43,** 363–374.

Jørgensen B. B. (1990) A thiosulfate shunt in the sulfur cycle of marine sediments. *Science* **249,** 152–154.

Kaplan I. R. and Rittenberg S. C. (1964) Microbiological fractionation of sulfur isotopes. *J. Gen. Microbiol.* **34,** 195–212.

Lasaga A. C. (1979) The treatment of multi-component diffusion and ion pairs in diagenetic fluxes. *Am. J. Sci.* **279,** 324–346.

Lasaga A. C. (1981) Influence of diffusion coupling on diagenetic concentration profiles. *Am. J. Sci.* **281,** 553–575.

Liang Y., Richter F. M., and Chamberlain L. (1997) Diffusion in silicate melts. III. Empirical models for multicomponent diffusion. *Geochim. Cosmochim. Acta* **61,** 5295–5312.

Liang Y., Richter F. M., Davis A. M., and Watson E. B. (1996a) Diffusion in silicate melts: I. Self diffusion in CaO-Al_2O_3-SiO_2 at 1500°C and 1GPa. *Geochim. Cosmochim. Acta* **60,** 4353–4367.

Liang Y., Richter F. M., and Watson E. B. (1996b) Diffusion in silicate melts. II. Multicomponent diffusion in CaO-Al_2O_3-SiO_2 at 1500°C and 1GPa. *Geochim. Cosmochim. Acta* **60,** 5021–5035.

McDuff R. E. and Ellis R. A. (1979) Determining diffusion coefficients in marine sediments: A laboratory study of resistivity techniques. *Am. J. Sci.* **279,** 666–675.

Monod J. (1949) The growth of bacterial cultures. *Ann. Rev. Microbiol.* **3,** 371–394.

Paytan A., Kastner M., Campbell D., and Theimens M. H. (1998) Sulfur isotope composition of Cenozoic seawater sulfate. *Science* **282,** 1459–1462.

Richter F. M. (1996) Models for the coupled Sr-sulfate budget in deep-sea carbonates. *Earth Planet. Sci. Lett.* **141,** 199–211.

Richter F. M. and DePaolo D. J. (1987) Numerical models for diagenesis and the Neogene Sr isotopic evolution of seawater from DSDP Site 590B. *Earth Planet. Sci. Lett.* **83,** 27–38.

Rudnicki M. D., Elderfield H., and Mottl M. J. (submitted) Pore fluid advection and reaction in sediments of the eastern flank, Juan de Fuca Ridge, 48°N. *Earth Planet. Sci. Lett.*

Shipboard Scientific Party. (1997) Methods. In *Proc. ODP Initial Reports* (eds. E. E. Davis, A. T. Fisher, J. V. Firth, et al.), Vol. 168A, pp. 35–45. Ocean Drilling Program.

Thomson R. E., Davis E. E., and Burd B. J. (1995) Hydrothermal venting and geothermal heating in Cascadia Basin. *J. Geophys. Res.* **100,** 6121–6141.

Toth D. J. and Lerman A. (1977) Organic matter reactivity and sedimentation rates in the ocean. *Am. J. Sci.* **277,** 465–485.

Tromp T. K., Van Cappellen P., and Key R. M. (1995) A global model for the early diagenesis of organic carbon and organic phosphorus in marine sediments. *Geochim. Cosmochim. Acta* **59,** 1259–1284.

Westrich J. T. and Berner R. A. (1988) The effect of temperature on rates of sulfate reduction in marine sediments. *Geomicrobiol. J.* **6,** 99–117.

Wheat C. G. and Mottl M. J. (1994) Hydrothermal circulation, Juan de Fuca Ridge eastern flank: Factors controlling basement water composition. *J. Geophys. Res.* **99,** 3067–3080.